

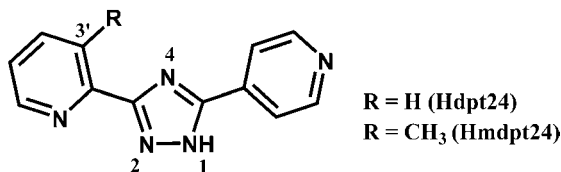
## Nonclassical Active Site for Enhanced Gas Sorption in Porous Coordination Polymer

Jian-Bin Lin, Jie-Peng Zhang,\* and Xiao-Ming Chen

MOE Key Laboratory of Bioinorganic and Synthetic Chemistry, State Key Laboratory of Optoelectronic Materials and Technologies, School of Chemistry and Chemical Engineering, Sun Yat-Sen University, Guangzhou 510275, China

Received February 3, 2010; E-mail: zhangjp7@mail.sysu.edu.cn

Porous coordination polymers (PCPs) have been of great interest for potential applications in gas storage<sup>1</sup> and separation.<sup>2</sup> It is well-known that large total pore volume is crucial for high gas uptake capacity, but small pore size elevates host–guest interactions and sorption amount at low relative pressures and/or high temperatures.<sup>3</sup> As total pore volume is determined by (usually proportional to) pore size, volume-size optimization can have a limited effect.<sup>4</sup> Alternatively, adsorption enthalpy may be enhanced by pore surface active sites such as coordinatively unsaturated metal centers<sup>5</sup> and amine groups,<sup>6</sup> which have been regarded to be useful for CO<sub>2</sub> and/or H<sub>2</sub>. Nevertheless, there are rare reports that have unambiguously proven the roles of active sites,<sup>5</sup> especially for organic functional groups, since pore surface engineering usually changes not only surface property but also pore volume, pore size, and even whole framework structure.<sup>7</sup> In this context, evaluation of weaker or nonclassical active sites is more challenging and intriguing.<sup>8</sup>



Our previous studies have demonstrated that metal azolate frameworks (MAFs) are favorable for controlling framework and pore surface structures.<sup>9</sup> The azolate nitrogen donors can be precisely controlled as coordination and guest binding sites.<sup>10</sup> Nevertheless, the roles of nitrogen donors in the resultant PCPs are not always straightforward. For example, crystallographic studies for the porous cuprous 3,5-diethyl-1,2,4-triazolate (MAF-2) loaded with different gases suggested that the coordinated nitrogens behave as the primary sorption sites, but detailed energy profiles are still unavailable without comparison with highly related materials.<sup>11</sup> Another type of puzzle is represented by a newly synthesized porous MAF [Co(dpt24)<sub>2</sub>] (**1**, MAF-25, dpt24 = 3-(2-pyridyl)-5-(4-pyridyl)-1,2,4-triazolate), in which the uncoordinated nitrogens are only partially exposed on the pore surface. To evaluate the activity of these nitrogens, we constructed an isostructural porous MAF [Co(mdpt24)<sub>2</sub>] (**2**, MAF-26, mdpt24 = 3-(3-methyl-2-pyridyl)-5-(4-pyridyl)-1,2,4-triazolate) for comparison. The methyl substituted new ligand was designed to block the suspected uncoordinated nitrogens.

The isostructural compounds crystallize in the trigonal space group  $R\bar{3}$ . Each octahedrally coordinated Co<sup>II</sup> ion is chelated by the 2-pyridyl and triazolate 2-nitrogens from two ligands in the *trans* configuration, and the two remaining coordination sites are occupied by 4-pyridyl nitrogens from adjacent units (Figure S1, Supporting Information),<sup>10b</sup> giving rise to a 4-connected three-

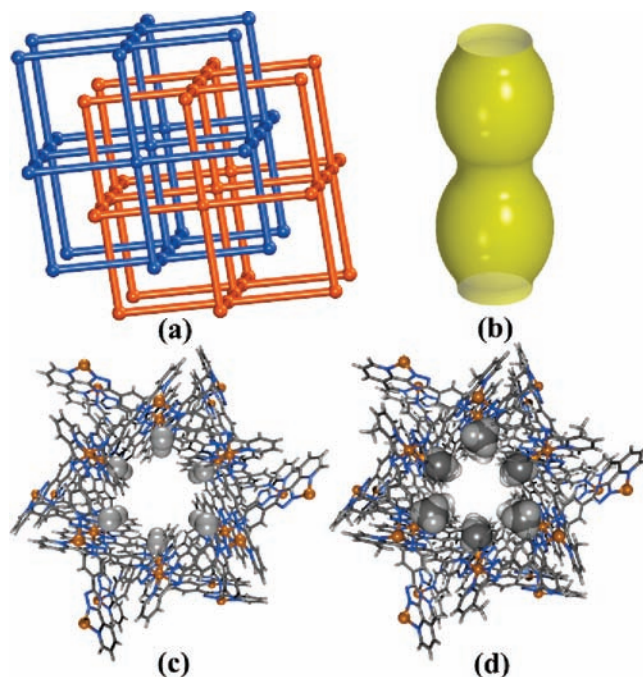


**Figure 1.** (a) Two-fold interpenetrating NbO net, (b) side-view of the 1D channel, and perspective views of the framework structures of (c) **1** and (d) **2** along the *c*-axes (the 3'-hydrogen atoms and -methyl groups on 2-pyridyl groups are highlighted in space filling modes).

dimensional (3D) NbO network.<sup>12</sup> After 2-fold interpenetration, there still remains 1D channels running along the *c*-axis, with alternating large cages and small necks (Figure 1).<sup>13</sup> The diameters of cage and neck in **1** are about 9.2 and 5.7 Å, respectively, taking into account the van der Waals radii. By incorporation of a methyl group in **2**, cage and neck diameters are reduced to ca. 7.7 and 5.2 Å, respectively.<sup>14</sup> The total solvent-accessible volumes are correspondingly reduced from 26.5% in **1** to 21.6% in **2**. The pore size differences suggest that **1** would have larger saturation adsorption capacity but lower adsorption enthalpy than **2**.<sup>15</sup>

The triazolate 1- and 4-nitrogens in **1** and **2** are uncoordinated. While the 4-nitrogens are completely covered by adjacent framework components, the 1-nitrogens are partially exposed on the pore surfaces. Due to the blockage of methyl group, the triazolate 1-nitrogens in **2** are much less exposed than those in **1** (Figure S2, Supporting Information). However, these partially exposed nitrogens may not be able to modulate the sorption properties, as their lone electron pairs do not point into the channels. Indeed, the solvent molecules in the two crystal structures are highly disordered, giving no specific information about host–guest interactions.

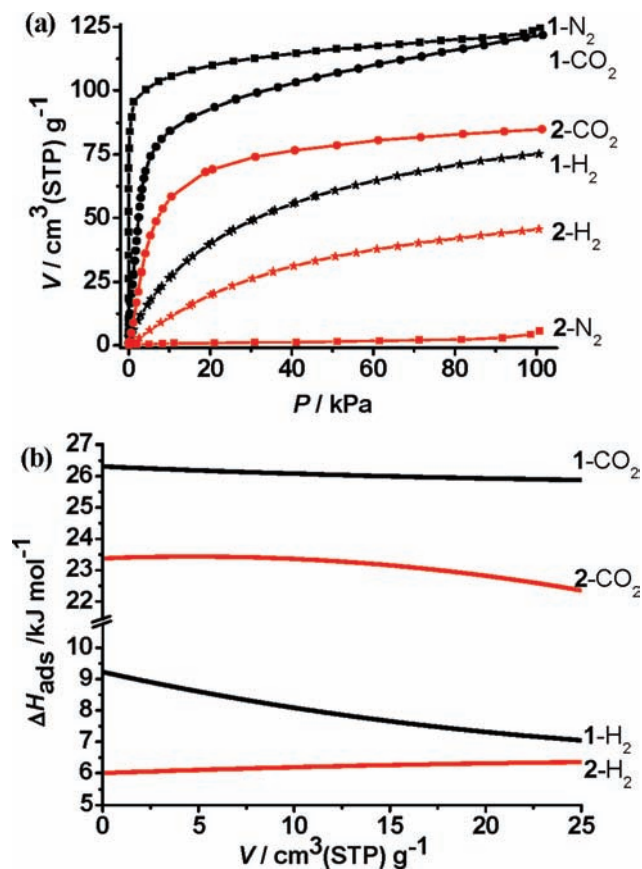


**Figure 2.** (a) Adsorption isotherms of  $\text{N}_2$  and  $\text{H}_2$  measured at 77 K and  $\text{CO}_2$  measured at 195 K, and (b) the adsorption enthalpies of  $\text{H}_2$  and  $\text{CO}_2$ .

Thermogravimetry analysis and variable-temperature powder X-ray diffraction show that **1** and **2** can be readily activated, keeping the host frameworks unchanged up to 440 °C in  $\text{N}_2$  and 370 °C in air, respectively (Figures S3, S4, and S5, Supporting Information), which are high values for PCPs.<sup>16</sup>

$\text{N}_2$  adsorption isotherms of activated **1** and **2** are measured at 77 K (Figure 2a). It shows type I isotherm with an apparent Langmuir surface area of 511  $\text{m}^2 \text{g}^{-1}$  for **1**. The adsorption amount of  $\text{N}_2$  at saturation is about 120  $\text{cm}^3(\text{STP}) \text{g}^{-1}$ , which corresponds to 8.1  $\text{N}_2$  per cage. In contrast, **2** only exhibits particle surface adsorption (5.7  $\text{cm}^3(\text{STP}) \text{g}^{-1}$  or 0.3  $\text{N}_2$  per cage at 1 atm), which may be derived from framework contraction or diffusion problem at low temperature<sup>17</sup> since the aperture size of **2** is larger than the kinetic diameter of  $\text{N}_2$  (3.64 Å).

The  $\text{H}_2$  uptake at 77 K and 1 atm for **1** and **2** are ca. 75 and 46  $\text{cm}^3(\text{STP}) \text{g}^{-1}$ , respectively (Figure 2a). This significant difference in  $\text{H}_2$  sorption capacity can be attributed to the void volume of **1** and **2**. Virial analysis<sup>18</sup> of the  $\text{H}_2$  adsorption isotherms measured at 77 and 87 K (Figures 2b, S6 and S7, Supporting Information) revealed that the adsorption enthalpy of **1** at zero surface coverage is 9.2(1)  $\text{kJ mol}^{-1}$ , which is higher than most PCPs with large pores.<sup>19</sup> However, the most intriguing result is that **2**, even though it has a smaller pore size, gives substantially lower adsorption enthalpies. The  $\text{H}_2$  adsorption enthalpy for **2** at zero surface coverage is 6.0(2)  $\text{kJ mol}^{-1}$ . To our knowledge, this is very unusual compared to previous reports, where smaller pores result in stronger overlapping potentials and thus higher adsorption energy.<sup>3a,4</sup>

In order to confirm the unusual gas attraction effect and sample quality after activation,  $\text{CO}_2$  sorptions were measured for **1** and **2**

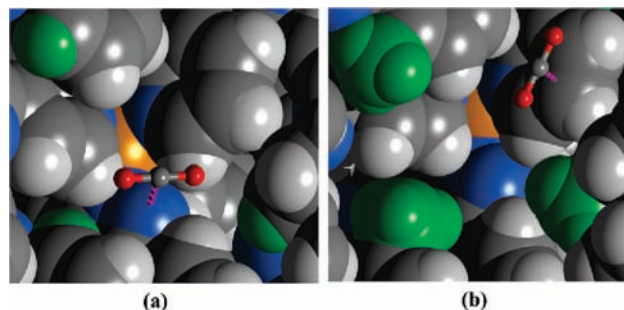


**Figure 3.** Preferential  $\text{CO}_2$  locations in (a) **1** and (b) **2** obtained from GCMC calculations (the 3'-hydrogen atoms and -methyl groups on 2-pyridyl groups are highlighted in green).

(Figure 2a) at 195 K, both of which exhibit type I isotherm with an apparent Langmuir surface area of 683 and 499  $\text{m}^2 \text{g}^{-1}$ , respectively. The saturation adsorption amount for **1** is about 117  $\text{cm}^3(\text{STP}) \text{g}^{-1}$ , corresponding to 7.9  $\text{CO}_2$  per cage; while the saturation adsorption amount for **2** is about 84  $\text{cm}^3(\text{STP}) \text{g}^{-1}$  and corresponds to 6.0  $\text{CO}_2$  per cage. The densities of  $\text{CO}_2$  in the channels of **1** and **2** at saturation are about 1.0 and 0.94  $\text{g cm}^{-3}$ , respectively, which are close to the density of liquid  $\text{CO}_2$  (1.10  $\text{g cm}^{-3}$ ), showing that the channels are effectively filled by  $\text{CO}_2$  molecules.

Furthermore,  $\text{CO}_2$  sorptions were performed at near room temperature, which would give more reliable results connected to crystal structures determined at room temperature. Virial analyses of the  $\text{CO}_2$  adsorption isotherms measured at 273 and 283 K (Figures 2b, S8 and S9, Supporting Information) also illustrate stronger binding ability for **1**. The enthalpies at zero coverage of **1** and **2** are 26.3(5) and 23.3(7)  $\text{kJ mol}^{-1}$ , respectively. These observations confirm that the isostructural framework **1** with larger pore size and total pore volume shows larger sorption amounts and higher enthalpies for both  $\text{H}_2$  and  $\text{CO}_2$ , which are very unusual and have been only observed for  $\text{H}_2$  adsorption in  $\text{Li}^+$ -doped PCP.<sup>19</sup> As discussed above, the unusual sorption behaviors can be only derived from the subtle difference on the exposure degree of uncoordinated nitrogens. In other words, even partially exposed uncoordinated nitrogens in **1** can lead to obvious improvement of adsorption enthalpy ( $>3 \text{ kJ mol}^{-1}$ ).

Due to the samples' poor single-crystallinity after removing guest molecules, we can not obtain the gas-loaded crystal structures. To further confirm the adsorption mechanism, grand canonical Monte Carlo (GCMC) simulations were employed to investigate the interactions between  $\text{CO}_2$  molecules and desolvated **1** and **2**. Simulations were performed for a model that includes electrostatic and Lennard–Jones 6–12 potential among the atoms in the system. The framework and the individual  $\text{CO}_2$  molecules were considered to be rigid. Interactions between  $\text{CO}_2$  molecules and framework were modeled with the UFF force fields (see the Supporting Information).<sup>20</sup>

$\text{CO}_2$  binding sites and corresponding enthalpies were obtained from the simulations. The calculations show that **1** possesses larger adsorption enthalpies than does **2**, which is in agreement with the experimental observations. The adsorption enthalpies at zero coverage are calculated to be 26.3 and 24.8  $\text{kJ mol}^{-1}$  in **1** and **2**, respectively. More interestingly, the preferential binding sites of the two structures are very different (Table S2, Supporting Information). In **1**, the  $\text{CO}_2$  molecule locates inside the large cage rather than the small aperture (Figure 3a), indicating that there is stronger binding interaction than the overlapping potentials. The  $\text{CO}_2$  molecule forms short contacts

with the uncoordinated triazolite 1-nitrogen by its electropositive carbon ( $C \cdots N = 3.57 \text{ \AA}$ ,  $O \cdots N = 3.76$  and  $3.77 \text{ \AA}$ ). The  $C \cdots N$  distance, being slightly larger than the sum of van der Waals radii of carbon ( $1.70 \text{ \AA}$ ) and nitrogen ( $1.55 \text{ \AA}$ ), suggests attractive interaction, presumably electrostatic in nature. The partially exposed nitrogen serves as an electronegative site. In **2**, the  $CO_2$  molecule is embedded in the small neck as expected (Figure 3b), which has strong overlapping potentials.  $CO_2$  is not likely interacting with the uncoordinated nitrogens as judged from the long  $C \cdots N$  separation ( $C \cdots N = 6.59 \text{ \AA}$ ,  $O \cdots N = 5.84$  and  $7.46 \text{ \AA}$ ), but forms short contacts with the 2-pyridyl carbons (shortest  $C \cdots C = 3.43 \text{ \AA}$ ). Further checking of other possible sorption sites verified that the  $CO_2$  molecule can not be located close to the uncoordinated triazolite 1-nitrogen, which should be ascribed to the blockage effect of methyl group (Figure S11, Supporting Information). Therefore, it is reasonable to conclude that the partially exposed uncoordinated nitrogen in **1** is able to provide a nondissociative interaction with gas molecules.

In summary, we have designed and synthesized two isomorphous PCPs with highly related pore characteristics, which represents an ideal system to investigate the effect of nonclassical active site for gas adsorption. Our results demonstrated that even partially exposed uncoordinated nitrogens can effectively enhance the gas binding affinity, which may have significant implication for future studies for engineering of new porous materials.

**Acknowledgment.** This work was supported by NSFC (Grant 20821001 & 90922031), “973 Project” (Grant 2007CB815302) and the Chinese Ministry of Education (Grant 109125).

**Supporting Information Available:** Crystallographic data, synthesis, EA, PXRD, additional structural plots, and additional sorption data. This material is available free of charge via the Internet at <http://pubs.acs.org>.

## References

- (1) (a) Murray, L. J.; Dincă, M.; Long, J. R. *Chem. Soc. Rev.* **2009**, *38*, 1294–1314. (b) Ma, S.; Zhou, H.-C. *Chem. Commun.* **2010**, *46*, 44–53. (c) Feréy, G.; Mellot-Draznieks, C.; Serre, C.; Millange, F.; Dutour, J.; Surble, S.; Margiolaki, I. *Science* **2005**, *309*, 2040–2042.
- (2) (a) Li, J.-R.; Kuppler, R. J.; Zhou, H.-C. *Chem. Soc. Rev.* **2009**, *38*, 1477–1504. (b) Couck, S.; Denayer, J. F. M.; Baron, G. V.; Remy, T.; Gascon, J.; Kapteijn, F. *J. Am. Chem. Soc.* **2009**, *131*, 6326–6327. (c) Guo, H.-L.; Zhu, G.-S.; Hewitt, I.-J.; Qiu, S.-L. *J. Am. Chem. Soc.* **2009**, *131*, 1646–1647. (d) Li, K.; Olson, D. H.; Seidel, J.; Emge, T. J.; Gong, H.; Zeng, H.; Li, J. *J. Am. Chem. Soc.* **2009**, *131*, 10368–10369.

- (3) (a) Jung, D.-H.; Kim, D.; Lee, T.-B.; Choi, S.-B.; Yoon, J.-H.; Kim, J.; Choi, K.; Choi, S.-H. *J. Phys. Chem. B* **2006**, *110*, 22987–22990. (b) Chun, H.; Dybtsev, D. N.; Kim, H.; Kim, K. *Chem.–Eur. J.* **2005**, *11*, 3521–3529. (c) Wong-Foy, A. G.; Matzger, A. J.; Yaghi, O. M. *J. Am. Chem. Soc.* **2006**, *128*, 3494–3495.
- (4) Lin, X.; Telepeni, I.; Blake, A. J.; Dailly, A.; Brown, C. M.; Simmons, J. M.; Zoppi, M.; Walker, G. S.; Thomas, K. M.; Mays, T. J.; Hubberstey, P.; Champness, N. R.; Schröder, M. *J. Am. Chem. Soc.* **2009**, *131*, 2159–2171.
- (5) (a) Caskey, S. R.; Wong-Foy, A. G.; Matzger, A. J. *J. Am. Chem. Soc.* **2008**, *130*, 10870–10871. (b) Dietzel, P. D. C.; Johnsen, R. E.; Fjellvåg, H.; Bordiga, S.; Groppo, E.; Chavan, S.; Blom, R. *Chem. Commun.* **2008**, 5125–5127. (c) Zhou, W.; Wu, H.; Yildirim, T. *J. Am. Chem. Soc.* **2008**, *130*, 15268–15269. (d) Lee, Y.-G.; Moon, H. R.; Cheon, Y. E.; Suh, M. P. *Angew. Chem., Int. Ed.* **2008**, *47*, 7741–7745. (e) Chen, B.; Ockwig, N. W.; Millward, A. R.; Contreras, D. S.; Yaghi, O. M. *Angew. Chem., Int. Ed.* **2005**, *44*, 4745–4749.
- (6) (a) An, J.; Geib, S. J.; Rosi, N. L. *J. Am. Chem. Soc.* **2010**, *132*, 38–39. (b) Demessence, A.; D’Alessandro, D. M.; Foo, M. L.; Long, J. R. *J. Am. Chem. Soc.* **2009**, *131*, 8784–8786. (c) Vaidyanathan, R.; Iremonger, S. S.; Dawson, K. W.; Shimizu, G. K. H. *Chem. Commun.* **2009**, 5230–5232. (d) Millward, A. R.; Yaghi, O. M. *J. Am. Chem. Soc.* **2005**, *127*, 17998–17999.
- (7) (a) Mulfort, K. L.; Hupp, J. T. *Inorg. Chem.* **2008**, *47*, 7936–7938. (b) Mulfort, K. L.; Hupp, J. T. *J. Am. Chem. Soc.* **2007**, *129*, 9604–9605.
- (8) (a) Higuchi, M.; Tanaka, D.; Horike, S.; Sakamoto, H.; Nakamura, K.; Takashima, Y.; Hijikata, Y.; Yanai, N.; Kim, J.; Kato, K.; Kubota, Y.; Takata, M.; Kitagawa, S. *J. Am. Chem. Soc.* **2009**, *131*, 10336–10337. (b) Yang, C.; Wang, X.; Omary, M. A. *J. Am. Chem. Soc.* **2007**, *129*, 15454–15455.
- (9) Zhang, J.-P.; Chen, X.-M. *Chem. Commun.* **2006**, 1689–1699.
- (10) (a) Zhu, A.-X.; Lin, J.-B.; Zhang, J.-P.; Chen, X.-M. *Inorg. Chem.* **2009**, *48*, 3882–3889. (b) Lin, J.-B.; Zhang, J.-P.; Zhang, W.-X.; Xue, W.; Xue, D.-X.; Chen, X.-M. *Inorg. Chem.* **2009**, *48*, 6652–6660.
- (11) (a) Zhang, J.-P.; Chen, X.-M. *J. Am. Chem. Soc.* **2009**, *131*, 5516–5521. (b) Zhang, J.-P.; Chen, X.-M. *J. Am. Chem. Soc.* **2008**, *130*, 6010–6017.
- (12) Liu, D.; Li, M.; Li, D. *Chem. Commun.* **2009**, 6943–6945.
- (13) Pan, L.; Olson, D. H.; Ciemmolowski, L. R.; Heddy, R.; Li, J. *Angew. Chem., Int. Ed.* **2006**, *45*, 616–619.
- (14) Chen, B.; Ji, Y. Y.; Xue, M.; Fronczek, F. R.; Hurtado, E. J.; Mondal, J. U.; Liang, C. D.; Dai, S. *Inorg. Chem.* **2008**, *47*, 5543–5545.
- (15) Patchkovskii, S.; Tse, J. S.; Yurchenko, S. N.; Zhechkov, L.; Heine, T.; Seifert, G. *Proc. Natl. Acad. Sci. U.S.A.* **2005**, *102*, 10439–10444.
- (16) Ma, S.; Wang, X.-S.; Yuan, D.; Zhou, H.-C. *Angew. Chem., Int. Ed.* **2008**, *47*, 4130–4133.
- (17) (a) Luo, J.-H.; Xu, H.-W.; Liu, Y.; Zhao, Y.-S.; Daemen, L.-L.; Brown, C.; Timofeeva, T.-V.; Ma, S.-Q.; Zhou, H.-C. *J. Am. Chem. Soc.* **2008**, *130*, 9626–9627. (b) Comotti, A.; Bracco, S.; Sozzani, P.; Horike, S.; Matsuda, R.; Chen, J.; Takata, M.; Kubota, Y.; Kitagawa, S. *J. Am. Chem. Soc.* **2008**, *130*, 13664–13672. (c) Chen, B.; Ma, S.; Zapata, F.; Fronczek, F. R.; Lobkovsky, E. B.; Zhou, H.-C. *Inorg. Chem.* **2007**, *46*, 1233–1236. (d) Cazorla-Amoros, D.; Alcaniz-Monge, J.; Linares-Solano, A. *Langmuir* **1996**, *12*, 2820–2824. (e) Garrido, J.; Linares-Solano, A.; Martin-Martinez, J. M.; Molina-Sabio, M.; Rodriguez-Reinoso, F.; Torregrosa, R. *Langmuir* **1987**, *3*, 76–81.
- (18) Dincă, M.; Dailly, A.; Liu, Y.; Brown, C. M.; Neumann, D. A.; Long, J. R. *J. Am. Chem. Soc.* **2006**, *128*, 16876–16883.
- (19) Yang, S.; Lin, X.; Blake, A. J.; Walker, G. S.; Hubberstey, P.; Champness, N. R.; Schröder, M. *Nat. Chem.* **2009**, *1*, 487–493.
- (20) Rappe, A. K.; Casewit, C. J.; Colwell, K. S.; Goddard, W. A.; Skiff, W. M. *J. Am. Chem. Soc.* **1992**, *114*, 10024–10035.

JA1009635